VOL. 15, NO. 5, MARCH 2020 ISSN 1819-6608
ARPN Journal of Engineering and Applied Sciences

www.arpnjournals.com

DESIGN AND SIMULATION OF A SPIRAL HYDRAULIC PUMP BASED ON MULTI-OBJECTIVE OPTIMIZATION

Eddisney Díaz[1], Carlos Trinchet[2] and Javier Vargas[3]
[1]Centro de Desarrollo de la Maquinaría Agrícola (CEDEMA), Holguín, Cuba
[2]Center for CAD / CAM Studies, University of Holguín, Cuba
[3]Faculty of Basic Sciences and Engineering, Macrypt Research Group, EYSI Study Group University of Llanos, Colombia
E-Mail: ediaz@cedema.co.cu

ABSTRACT

Hydraulic pumps have played a decisive role in the development of humanity. Clean and accessible water is an essential ingredient for a healthy life all over the world. Renewable energies are called to move the world; you can no longer rely on oil for much longer. Autonomous spiral pumps have been built that work with the kinetic energy of the water flow. The aim of this research was to develop a procedure for the optimal design of the spiral pump. The numerical simulation of the model is performed in a CAE environment, using octave software. The design of the pump elements and the simulation of their mechanical properties are performed with CAD tools from software. The design and validation developed ensure an optimal design, which facilitates the task of decision making for manufacturing.

Keywords: hydraulic pump, spiral pump, multi-objective optimization, CAD simulation, computational numerical simulation.

1. INTRODUCTION

Bombs have played and continue to play a decisive role in the development of humanity (Vargas, Clavijo, and Torres Gómez 2016). It is impossible to imagine modern industrial processes and life in large cities without the participation of these teams (Vargas *et al.* 2016). The search for profitable pumps is a research priority throughout the world (Thompson *et al.* 2011). The spiral pump is a sustainable, economical and relevant pump in different industrial and commercial works. The spiral pump was created in 1746 by H. A. Wirtz in Zurich-Switzerland, who took Archimedes' screw and hydraulic wheel as a reference. (Huol, I, and Zhou 2014) (Tang *et al.* 2017) The spiral pump is formed by a tube rolled in a horizontal axis which rotates by means of the blades that capture the kinetic energy of the river or ditch (Divakar and Rajesh 2016) (Andrade *et al.* 2008). The outer end of the tube is open, and is immersed in the water once per revolution.

At each 360 degree turn the spiral is filled with water, and another part is filled with air. With each revolution of the wheel, the air is compressed in each circle of the spiral. In this way, a height of pressure is added that causes the water to expel in the inner end of the rolled tube that coincides with the center of the spiral, this pressure obtained is due to two principles, the hydrostatic pressure and the push of the air bubble.

One of the variants of this type of pump is the Barsha pump, developed by the Dutch company a Qysta. The pump is a water wheel that is placed on a floating platform in a river and uses the kinetic energy of water to pump (Denchfield, Marth, and Shelmerdine 2007). The water through hoses. Its operation does not use any type of fuel or electricity; it uses the kinetic energy of the water flow to move the wheel (Khattak *et al*. 2016).

The following is a list of some of the works to be carried out in the course of this research. These contributed to the state of the art of the proposed technological development.

Basunia and other (2016) developed a hand pump with a plastic drum as support structure for the coil. They made a physical model of the prototype, to understand the pumping action of the pump. They found that the maximum discharge is 9.0 liters per minute with a tilt angle of 20° through the discharge pipe. The calculated human power to manually spin the pump was approximately 11.36 W (0.15 HP) within five minutes of rotation. The maximum human power is 75 W in eight working hours.

Singh and other (2016), propose a multiple spiral wound tube pump methodology, this model is a further modification stage in the existing research with three spiral tubes wound in the same frame at 120° from the inlet ends and connected to a common outlet tube at the swivel joint, resting on the vertical axis. The wheel rotates with the help of the chain transmission and sprocket, which requires an initial start with a handle. The 3-tube spiral concept improved the efficiency of the pump by reducing the possibilities of empty tube rotations and transferring more water, with three packs in a single rotation.

S. N. Waghmare, M. M. Mestri, P. V. Lavekar, T. S. Misal and P. C. Nalawade proposed a model that is composed of chip raw materials and is purely independent of power or fuel supply. The different results were calculated with the help of different parameters such as discharge, head, wheel structure rpm, applied p ar, pipe size, etc. The analytical study showed the effect of the wheel size on the discharge, the effect of the torque applied on the discharge, and the effect of the torque applied on the head etc. That the spiral tube water wheel pump is the best replacement for the current pump, as it can be used in rural areas where electricity decomposition frequently occurs.

Waghmare and others (2015), proposed a model to obtain the desired height and discharge of water. Where the pump was driven by chain, so it was added the manual operation to run the pump. Regarding the use of 3D

ARPN Journal of Engineering and Applied Sciences

simulation, Shahrbanouzadeh, Barani, and Shojaee (2015) used the simulation of flow through the foundations of a dam using the finite element technique. The model found made it possible to predict the piezometric height of the head and infiltrations through the foundations of a concrete dam. The results obtained from this study demonstrated that finite element models produce spatial and temporal variations of variables.

Patil, N. R., Gaikwad, S. R., Navale, R. A., & Sonawane (2014), designed and constructed a manually operated experimental configuration to analyze the performance of the spiral pump in different parameters. Parameters considered are immersion ratios, rotation speed and coil layers. For a wheel diameter configuration of 0.8 m with 7 coils, the maximum height obtained is between 4.3 and 5 m with a maximum flow of 1200 l/h for a single layer and 2280 l/h for the double layer of the coil, with an efficiency range of 20 % to 74 %. As can be seen in this investigation, the discharge flow increases almost twice for a two-layer pump, in this case when talking about layers refers to the number of spirals of the pump, so it is an important design parameter to take into account.

Kojima, Yamazaki, and Edge (2009), determined by experimentation the inherent pulsation power generated by a hydraulic pump, using both the "pulsation intensity tech-nique" method and a theoretically derived conversion equation to eliminate the influence of a hydraulic circuit on the measurement. For this purpose, the pump pulsation source was modelled and the source pulsation simulation was obtained from the axial piston pump test. They studied the hydraulic piping system, the pressure and flow pulsations in a reference pipe and its progressive and in the investigation the different models that evaluate the operation of the spiral pumps were analyzed; which will be taken into account for the optimization of the work process of the same one. By means of external analysis, the mathematical model is defined; by means of internal analysis, the rational organization of the calculation procedures that allow determining the optimal solutions for the design process proposed in the research is specified (Kroes, Franssen, and Bucciarelli 2009).

2. PRINCIPLE OF OPERATION

This pump is simple in both construction and operation. It consists of a length of flexible pipe coiled in a spiral shape in a plane perpendicular to the axis of rotation of the pump, which is partially submerged in water, with the axis of the pump parallel to the surface of the water. The outer end of the spiral is left open and this forms the pump inlet. The other inner end of the spiral tube is connected via a rotating hydraulic seal to the supply or discharge tube. The blades are responsible for capturing the kinetic energy of the river to rotate the pump, as the packages are moved within the spiral by the effect of rotation, the compression of the air packages causes the height of the water column in each spiral to gradually increase, each turn of the pipe functions as a U-gauge and the differential of the pressure deltas in each spiral is added and provides the fluid with a positive net head, which then depends on the spiral number of the pump and is the one that will allow the water to be expelled by the discharge hose to the field.

2.1 Application of the analysis and synthesis of engineering systems.

In any process, system analysis begins by considering the input and output magnitudes which, together with the magnitudes representing the internal state of the system, constitute the main indicators of all systems [5].

Therefore, the multi-criteria optimisation task is replaced by the multi-task solution with a single objective that includes each and every objective and constitutes an approximation to the multi-objective value function. The function is presented in equation 1.

$$Z = \max[w_1 (f_{Qp} - f_{Qp}\, d), w_2 (f_H - f_H\, d)] \quad (1)$$

regressive wave components, the pulsation power in the reference pipe and its progressive and regressive wave components. Finally, they propose a standard test procedure

^{f}Qp is the discharge flow function.

to experimentally determine the pulsation power inherent in a hydraulic pump source.

3. MATERIALS AND METHODS

f_H is the discharge height function.
$f_i\, d$ is the desired values for each target function.
w_i are the weight values for each target function.

The proposed restrictions are given by the Outside Loop Diameter (m), Inside Hose Diameter (m3), Hose Thickness and Revolutions (min-1). In Table-1, the restrictions are presented.

r: Radius: radius of the helical pipe.
$Lw1$: Length at which the pipe remains submerged at the inlet.

In (3) the equation without dynamic losses is presented:

Table-1. Strouhal number for different geometric cases

PARAMETERS	RESTRICTIONS
Outside Loop Diameter (m)	$[1,2 \geq x_1 \leq 1,8]$
Inside Hose Diameter (m^3)	$[0,0166 \geq x_2 \leq 0,0554]$
Hose Thickness (m)	$[0,0017 \geq x_3 \leq 0,0038]$
Revolutions (min^{-1})	$[5 \geq x_4 \leq 15]$

$$L_{w1} = \theta_1 R \quad (2)$$

Where:

θ_1: Angle traveled by the inlet mouth into the water with respect to the center of the pump.

R: Distance from the center of the wheel to the middle line of the external loop of the pump.

4. RESULTS AND DISCUSSIONS

In order to determine the different variants of the geometric and functional parameters of the spiral pumps, the values of the efficiency indicators of each one of the pump configurations that were defined beforehand are identified. They were evaluated at 3 levels at which the pump would be submerged, for a value of: 150º, 140º, 130º. To determine the values or ranges of the variables at which the flow equation was to be evaluated, they are based on the bibliographic review.

4.1 Discharge flow from the pump

G.H. Mortimer and R. Annable [6] in their research determine an equation (2) for the discharge flow of the spiral pump, which is one of the efficiency indicators to be obtained.

$$Q_p = N_s \pi r^2 L_{w1} \qquad (3)$$

Where:

Ns: Number of revolutions of the pump.

The discharge flow rate was determined for each external diameter of the pump, varying the internal diameter of the hose with its thickness and for each of the working revolutions of the pump in the range chosen above, for the three positions defined to submerge the pump. It was found that when $\theta 1$ it is longer and therefore the length at which the pump is submerged, the discharge flow of the pump increases.

For each external diameter of the pump, the corresponding heights and numbers of spirals were obtained for each one of the internal diameters of the hose acquired from the catalogue.

Figure-1 shows the head and flow value for a pump outside diameter of 1.8 m, which is the best value for the pump efficiency indicators, evaluated for the three angles at which the pump can be submerged. Corroborating that for a $\theta 1$ =150º better values of flow are obtained and that for a hose of internal diameter of 0,028 m the values of head and flow are balanced, reason why it is determined that it is a suitable solution for the design of the pump.

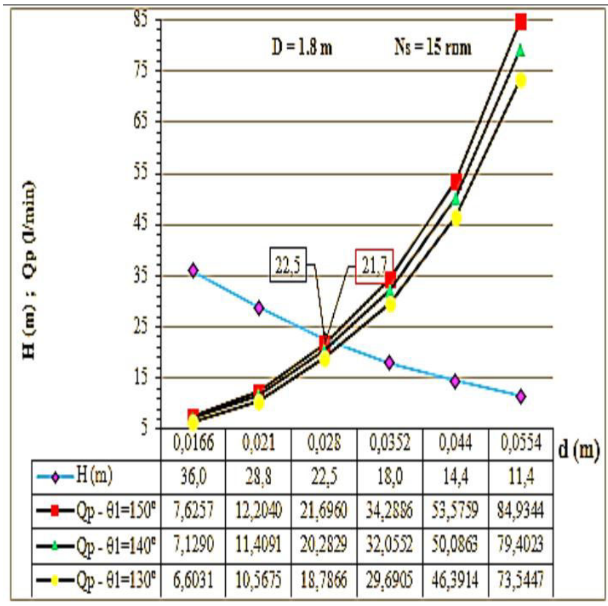

	0,0166	0,021	0,028	0,0352	0,044	0,0554
H (m)	36,0	28,8	22,5	18,0	14,4	11,4
Qp - θ1=150º	7,6257	12,2040	21,6960	34,2886	53,5759	84,9344
Qp - θ1=140º	7,1290	11,4091	20,2829	32,0552	50,0863	79,4023
Qp - θ1=130º	6,6031	10,5675	18,7866	29,6905	46,3914	73,5447

Figure-1. Height and flow with respect to the inner diameters of the hoses for each θ of the pump.

4.2 Multi-objective numerical simulation of efficiency indicators

The multi-objective optimization of the mathematical model was carried out by the method of Exploration of Nonlinear Programming with restrictions. The computational simulation, according to the model of the Tchebycheff Program, was implemented. A series of optimal variants of the efficiency indicators and the variables that govern the process were obtained for the design of the spiral pump. Figure-1 shows the front of Pareto of the not inferior solutions.

For the design, the efficiency indicators were prioritized, in order to have a set of optimum solutions for the design of the spiral pump. The design and numerical simulation of its mechanical properties were carried out with the results obtained by means of the multi-objective optimisation model.

Once the optimum values for pump operation and the corresponding geometrical values have been obtained, the 3D design of all pump parts is carried out in the CAD software. The subassemblies and the general assembly of the pump are generated and the technical documentation of the pump is made, the subassemblies and the general assembly of the pump are generated and the technical documentation of the pump is made. Figure-3 shows the CAD design.

ARPN Journal of Engineering and Applied Sciences

www.arpnjournals.com

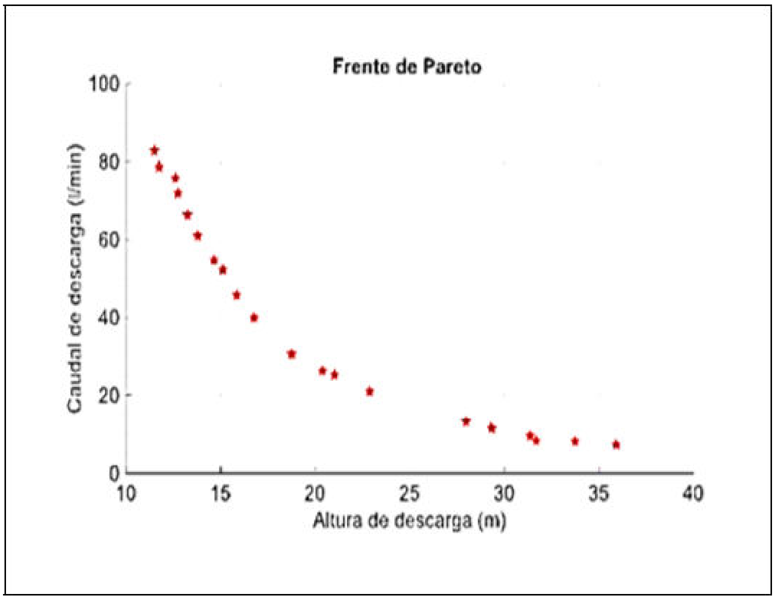

Figure-2. Front of Pareto of the not inferior solutions.

Table-2 shows the results of the computational simulation, the result values in red are the optimal values for the design. The optimum points for hydraulic turbine design are identified in rows 5, 6, 8 and 10 of table.

Table-2. Multi-objective optimization results.

#	H	**Qp**	**D**	**d**	**e**	**Ns**
	(m)	**(l/min)**	**(m)**	**(m)**	**(m)**	**(min^{-1})**
1	31,36	9,73	1,79	0,019	0,0018	14,61
2	27,96	13,40	1,80	0,022	0,0017	14,61
3	29,32	11,72	1,79	0,020	0,0018	14,62
4	14,65	54,74	1,79	0,045	0,0019	14,62
5	20,38	26,43	1,79	0,031	0,0019	14,63
6	22,87	21,08	1,80	0,028	0,0018	14,61
7	16,77	40,00	1,79	0,038	0,0022	14,62
8	18,75	30,64	1,79	0,033	0,0023	14,62
9	15,11	52,38	1,80	0,044	0,0018	14,63
10	21,02	25,33	1,79	0,030	0,0017	14,62

ISSN 1819-6608
ARPN Journal of Engineering and Applied Sciences

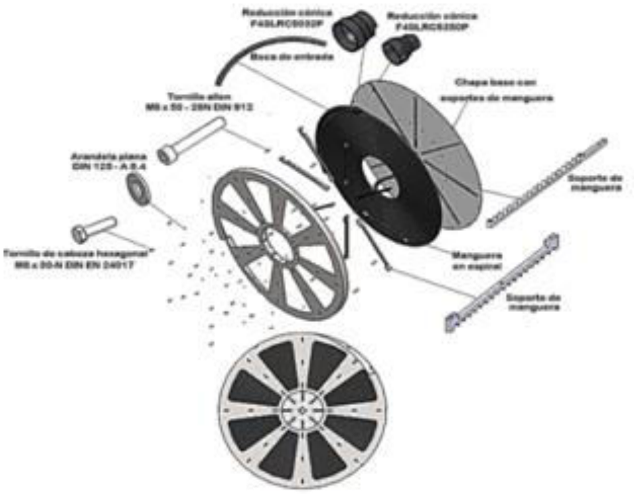

Figure-3. Exploded view of the pump spiral design.

The shafts are in charge of supporting the weight of the pump and the fastening of the spirals. These allow the rotation of the same for its correct operation, the material of all the components is stainless steel AISI 304. Figure-4 shows the CAD design.

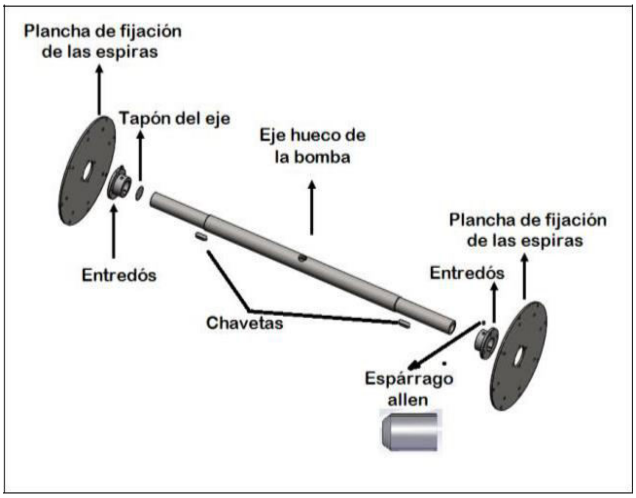

Figure-4. Exploded view of the pump spiral design.

The blades are responsible for capturing the kinetic energy of the river and rotating the pump. It is made of a 1.5 mm thick sheet of stainless steel AISI 304 because it must be resistant to corrosion as it will be in direct contact with water for long hours of work. It must resist the impact of the water without being deformed and at the same time be light. Figure-5 shows the design of the blades.

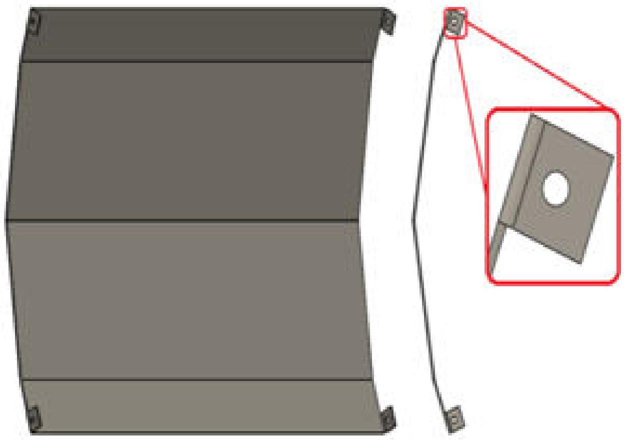

Figure-5. Exploded view of the pump spiral design.

4.3 Numerical simulation of mechanical properties

In the simulation to check the mechanical properties of the pump components, a static study is carried out of the assemblies support, bearing support and pump shaft, on which all the weight and efforts of the pump fall. The assembly will be taken as a rigid solid for that particular moment, assuming the calculated dimensions. A force of 300 kg is applied to it, which is a greater weight than the real weight of the other components.

The general result of the stress state of the model is expressed according to the stress of Von Mises as shown in Figure-6. The maximum stress of Von Mises is compared with the elastic limit of the material of the part, to know if the plastic deformations exceed the deformation limit of the material. The maximum tension obtained was 45.3 MPa and the elastic limit of the material Steel AISI 304 is 207 MPa, so the maximum tension of Von Mises supported by the model is less than the elastic limit of the material; so it perfectly resists these values of plastic deformation.

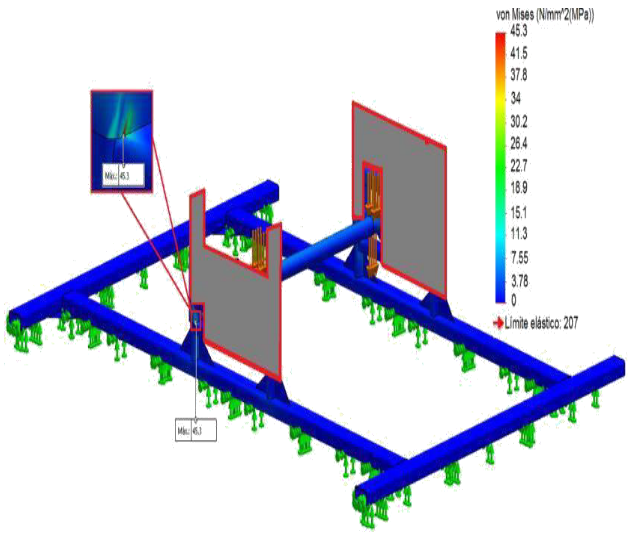

Figure-6. Exploded view of the spiral pump design.

Figure-7 shows the maximum displacements of the model obtained in the simulation, with a value of 0.15 mm, these displacements are very small and do not influence the correct operation of the pump. The maximum value of the unit deformations produced by the applied external forces is also appreciated, with a value of 0.00015 ESTRN, which is a small value within the deformation limits.

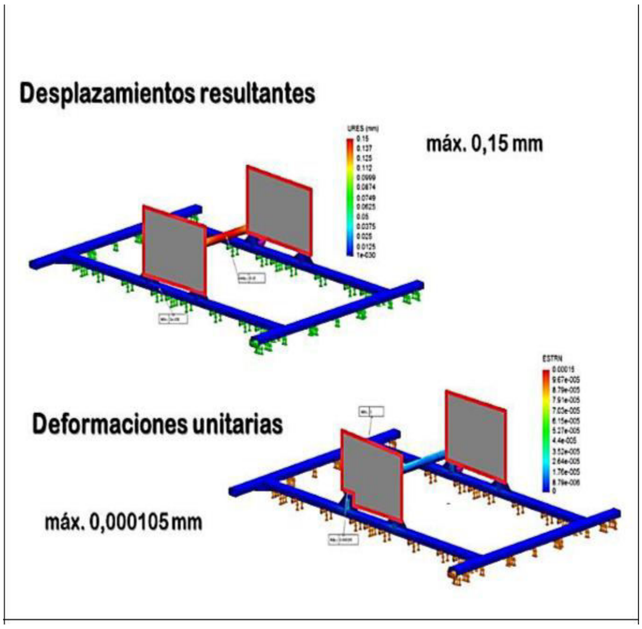

Figure-7. Exploded view of the spiral pump design.

The appropriate safety factor must be greater than 1. For the design of the hydraulic pump the safety factor was 4.56. Therefore the model complies with the safety factor parameter. This allows to reduce the geometry and to diminish weight in the pump for a better manipulation of the sam. Figure-8 shows the simulation carried out.

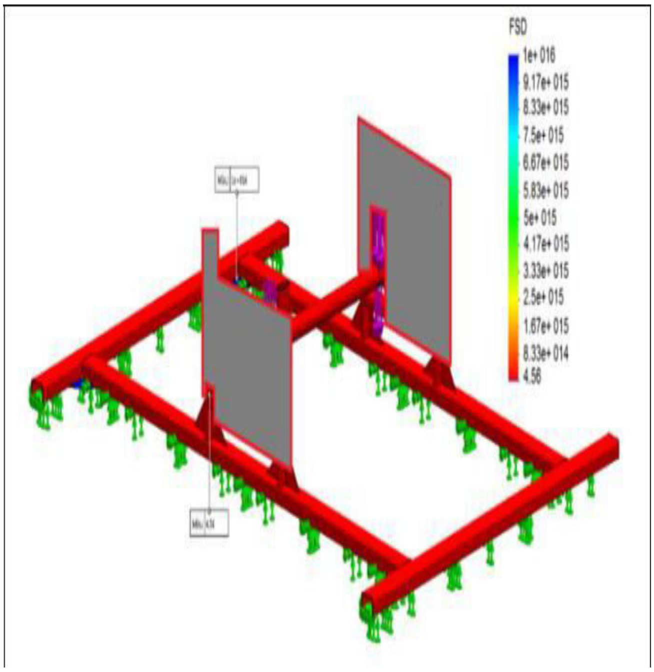

Figure-8. Simulation of the safety factor of the model.

4.4 Determination of the logical consistency of the result

Table-3 shows the values obtained in the investigation and they are compared with those obtained from the manufactured pumps and other investigations found according to the bibliographic review, this allows appreciating the logical consistency of the assumed solution.

Table-3. Comparison of the constructive and functional parameters of the pump design.

Parameters	Calculated spiral pump		Commercial and conventional spiral pump	
	Alternative 1	Alternative 2	Alternative 1	Alternative 2
Diameter of pump outer loop (m)	1,7966	1,8000	1,8000	1,8000
Inner loop diameter (m)	0,5980	0,6000	86,3600	0,8123
Diameter of pipe (m)	0,0313	0,0280	0,0318	0,0191
Number of coils	18,0000	19,9800	13,0000	21,0000
Pipe thickness (m)	0,0019	0,0018	0,0021	0,0022
Speed (rpm)	14,6000	14,6000	12,0000	12,0000
Discharge flow rate (l/min)	26,4300	21,0870	30,5800	17,0000
Discharge height (m)	20,3800	22,8700	12,0000	12,0000

In this case, two of the results obtained through multi objective simulation were compared with the two spiral pump prototypes constructed and evaluated in the specialized literature. It can be seen how in conventionally constructed pumps one of the efficiency indicators deteriorates more than the other, and in those obtained, by means of multi objective simulation, the values of the indicators are equivalent, since the algorithm does not seek an optimal solution, but a set of possible solutions of equivalent quality, which gives validity to the use of this tool at the time of conceiving a product. It should be noted that in this research only the optimization of the spiral is submitted, the rest of the elements of the pump are assumed in ranges obtained in other researches.

5. CONCLUSIONS

The development of the fundamentals of Analysis and Synthesis of Engineering Systems for the preparation and decision making under multiple criteria, in the design activity of the spiral pump, allows obtaining a multi objective mathematical model that bases a reasonable compromise between the efficiency indicators and the assumed decision variables.

Mathematical modeling allows us to provide solutions that, although not unique, can be considered rational, based on the basis made to define the technical and dimensional requirements, the numerical simulation of their mechanical properties and the design of the spiral pump.

It was determined that the model designed complies with the safety factor equvialente 4.56. The maximum voltage obtained was 45.3 MPa finding that the material Steel AISI 304 is suitable for the manufacture of the turbine.

REFERENCES

Andrade Aron, José Biscegli, José Eduardo Sousa, Yukio Ohashi, and Yukihiko Nosé. 2008. Flow Visualization Studies to Improve the Spiral Pump Design. Artificial Organs. 21(7): 680-85. Retrieved (https://doi.org/10.1111/j.1525-1594.1997.tb03722.x).

Basunia M. A., Nora Shafitri Binti Abdul Wahid, Maziri Bin D. H. Morsidi and Ahmed S.Bi. H. A. Rahman. 2016. A Manually Operated Coiled Tube Pump Using Plastic Drum as a Coil Supporting Structure. Agricultural Engineering International: CIGR Journal 18(4):81–86.

Denchfield, Sally, Reinhard Marth and Bob Shelmerdine. 2007. Stream Wheels for Applications in Shallow and Deep Water. 32nd IAHR Conference 2007, Venice, Italy, 01 - 06 Jul 2007. (1): 1-9.

Divakar Praveen and Harshal Rajesh. 2016. Spiral Tube Water Wheel Pump. International Journal on Recent and Innovation Trends in Computing and Communication. 4(4): 137-39.

Huol Youwen, Zaibing Pan I and Wenchao Zhou. 2014. Effects of Centrifugal Pump Volute. pp. 1-5 in 2014 ISFMFE - 6th International Symposium on Fluid Machinery and Fluid Engineering.

Khattak M. A., N. S.Mohd Ali, N. H.Zainal Abidin, N. S. Azhar and M. H. Omar. 2016. Common Type of Turbines in Power Plant: A Review. Journal of Advanced Research in Applied Sciences and Engineering Technology. 3(1): 77-100.

Kojima Eiichi, Toru Yamazaki, and Kevin Edge. 2009. Development of Standard Testing Procedure for Experimentally Determining Inherent Source Pulsation Power Generated by Hydraulic Pump. International Journal of Fluid Power. 10(1): 27-35.

Kroes Peter, Maarten Franssen, and Louis Bucciarelli. 2009. Rationality in Design. pp. 565-600 in Handbook of the Philosophy of Science, edited by A. B. T.-P. of T. and E. S. Meijers. Amsterdam: North-Holland. Retrieved (http://www.sciencedirect.com/science/article/pii/B9780444516671500252).

Patil N. R., Gaikwad S. R., Navale R. A. & Sonawane D. S. 2014. Design, Manufacturing and Performance Analysis of Spiral Coil Pump. N Applied Mechanics and Materials 446: 549-52.

Singh, Sameer, Tuhin Srivastava, Nitish Aarya, Sarthak Mittal and Rishab Singh. 2016. Performance and Analysis of Triple Scoop Spiral Pump. Vth International Symposium on Fusion of Science & Technology. 18(22): 530-32.

Tang Xiaoyan, Zhong Yun, Junrui Xu and Chao Cai. 2017. The Design of the Magnetic and Hydraulic Suspension System on an Axial Blood Pump and the Analysis of Its Mechanical Properties. pp. 1994-97 in 2017 IEEE 2nd Advanced Information Technology, Electronic and Automation Control Conference (IAEAC).

Thompson, Phillip L., Sonya Milonova, Meghan Reha, Faisal Mased and Ian Tromble. 2011. Coil Pump Design for a Community Fountain in Zambia. International Journal for Service Learning in Engineering. 6(1): 33-45.

Vargas, Javier Andrés, Fabián Velásquez Clavijo and Camilo Torres Gómez. 2016. Desarrollo Del Prototipo de Un Hidrogenerador Eléctrico Como Alternativa de Generación de Energía Limpia En Zonas Rurales Development of the Prototype of an Electric Hydro Generator as an Alternative for Generating Clean Energy in Rural Areas. Ingeniare. 12(20): 91-101.

Vargas Javier, Jeison Arango, Manuel Salazar, Hector Torres and Liliana Herrera. 2016. Prototipo Mecanico Para La Transformacion de Energía Hidraulica En Energía Electrica. 10(1).

Waghmare S. N., M. M. Mestri, P. V. Lavekar, T. S. Misal and P. C. Nalawade. 2015. Manually Operated Spiral Tube Water Wheel Pump. International Research Journal of Engineering and Technology (IRJET). 2(1): 167-69.